Chemical Platinization and its Effect on Excitation Transfer Dynamics and P700 Photooxidation Kinetics in Isolated Photosystem I

James W. Lee,* Ida Lee,* Philip D. Laible,‡ Thomas G. Owens,‡ and Elias Greenbaum*
*Oak Ridge National Laboratory, Oak Ridge, Tennessee 37831-6194; and ‡Section of Plant Biology, Cornell University, Ithaca, New York 14853 USA

ABSTRACT Isolated photosystem I (PSI) reaction center/core antenna complexes (PSI-40) were platinized by reduction of $[PtCl_6]^{2-}$ at 20°C and neutral pH. PSI particles were visualized directly on a gold surface by scanning tunneling microscopy (STM) before and after platinization. STM results showed that PSI particles were monomeric and roughly ellipsoidal with major and minor axes of 6 and 5 nm, respectively. Platinization deposited ~1000 platinum atoms on each PSI particle and made the average size significantly larger (9 × 7 nm). In addition to direct STM visualization, the presence of metallic platinum on the PSI complexes was detected by its effect of actinic shading and electrostatic shielding on P700 photooxidation and $P700^+$ reduction. The reaction centers (P700) in both platinized and nonplatinized PSI-40 were photooxidized by light and reduced by ascorbate repeatedly, although at somewhat slower rates in platinized PSI because of the presence of platinum. The effect of platinization on excitation transfer and trapping dynamics was examined by measuring picosecond fluorescence decay kinetics in PSI-40. The fluorescence decay kinetics in both platinized and control samples can be described as a sum of three exponential components. The dominant (amplitude 0.98) and photochemically limited excitation lifetime remained the same (16 ps) before and after platinization. The excitation transfer and trapping in platinized PSI-40 was essentially as efficient as that in the control (without platinization) PSI. The platinization also did not affect the intermediate-lifetime (400–600 ps) and long-lifetime (>2500 ps) components, which likely are related to intrinsic electron transport and to functionally uncoupled chlorophylls, respectively. The amplitudes of these two components were exceptionally small in both of the samples. These results provide direct evidence that although platinization dramatically alters the photocatalytic properties of PSI, it does not alter the intrinsic excitation dynamics and initial electron transfer reactions in PSI.

INTRODUCTION

Functional interaction of biological systems with those of nonbiological origin is an interesting, although relatively unexplored, area of biophysical research. Such interactions have been discussed philosophically (Hoffmann, 1990) and with specific examples (Mann et al., 1993). Metallic platinum is an active catalyst for photosynthetic production of molecular hydrogen in chemically platinized thylakoids (Greenbaum, 1985; Hitchens et al., 1991). Chemical platinization was achieved through the redox reaction of water-soluble hexachloroplatinate with dihydrogen:

$$[PtCl_6]^{2-} + 2H_2 \rightarrow Pt\downarrow + 6Cl^- + 4H^+.$$

With essentially the same redox reaction, platinization has also been achieved by photoreduction of $[PtCl_6]^{2-}$ by photosystem I (PSI) instead of H_2 (Greenbaum, 1988). Metallic (insoluble) platinum has been identified in photosynthetically platinized thylakoids by x-ray fluorescence analysis (Lee et al., 1994). In platinized thylakoids, metallic platinum in direct contact with PSI catalyzed H_2 production through reduction of protons by PSI (Greenbaum, 1985, 1988, 1989).

In addition to photocatalysis, another important application of platinization is in the area of bioelectronics. Using thylakoids and isolated reaction centers, for example, several research groups have constructed photoelectrochemical cells (Lemieux and Carpentier, 1988; Sanderson et al., 1987; Okano et al., 1984). In these earlier studies, however, diffusible redox mediators such as 2,5-dichlorobenzoquinone, phenazine methosulfate, or methyl viologen were used to couple the photochemical reaction to external electrodes. Because of the relatively slow diffusional motion of the redox mediators, all of these studies suffered a common problem of efficiency and response time, as pointed out by Katz et al. (1989) in a study using bacterial reaction centers. We believe that this problem can be solved by making direct electrical contact with terminal electron carriers of reaction center complexes using platinum particles, because metallic platinum is not only an active catalyst but also a good conductor. Platinum has a useful property in that some of its compounds (such as $[PtCl_6]^{2-}$) are water soluble and can be reduced (by H_2 or by electrons from PSI) to metallic platinum at ambient temperature and pH 7. This property makes it suitable for depositing fine metallic platinum particles onto biological systems while preserving their functionality.

PSI is one of the fundamental energy-transducing components of photosynthesis, which converts sunlight into electrochemical energy through efficient energy transfer

Received for publication 3 June 1994 and in final form 1 January 1995.

Address reprint requests to Dr. Elias Greenbaum, Oak Ridge National Laboratory, P.O. Box 2008, Bldg. 4500-N, Oak Ridge, TN 37831-6194. Tel.: 615-574-6835; Fax: 615-574-6843; E-mail: exg@ornl.gov.

0006-3495/95/08/652/08 $2.00

among antenna pigments coupled to photochemistry in the reaction center. The photochemical reaction results in charge separation and vectorial electron transport from the special pair of reaction center pigments (P700) to a terminal electron acceptor F_{AB} via intermediate acceptors A_o, A_1 and F_x (Golbeck and Bryant, 1991; Krauss et al., 1993). By the technique of chemical platinization, metallic platinum particles have been deposited on the reducing site (F_{AB}) of PSI in thylakoid membranes, and vectorial photosynthetic current has been detected through the metallic platinum particles (Greenbaum, 1992).

The focus of the work described in this paper is the scanning tunneling microscopic and spectroscopic characterization of chemical platinization and its effect on PSI function. We have examined the effect of platinization by measuring excitation transfer dynamics and P700 photooxidation kinetics. The key finding of this work is that platinization does not degrade the intrinsic electron transfer function of the photosynthetic reaction centers. Chemical platinization has potential as a new biophysical technique for direct electrical contact with emergent electrons from the PSI reaction center.

MATERIALS AND METHODS

Isolation of photosystem I particles

Thylakoids were isolated from spinach leaves using the procedure described by Reeves and Hall (1980). Photosystem I reaction center/core antenna complexes containing ~40 chlorophylls (chls) per photoactive P700 (PSI-40) were isolated from the thylakoids using the technique of detergent (Triton X-100) solubilization and hydroxylapatite column purification (Lee et al., 1992; Lee, 1993). PSI-40 was eluted in a buffer (0.2 M phosphate, pH 7.00, containing 0.05% Triton X-100). P700 concentration was determined using chemically induced absorbance change at 697 nm (Markwell et al., 1980) and a differential extinction coefficient of 64 M^{-1} cm^{-1} (Hiyama and Ke, 1972). Chlorophyll content was determined in 90% acetone extract (Jeffery and Humphrey, 1975). Absorbance spectra of the samples were measured with a UV-VIS scanning spectrophotometer (UV-2001PC, Shimadzu Corporation, Kyoto, Japan).

Chemical platinization of PSI-40

The PSI-40 eluate containing 47 μM chl was used for chemical platinization with 2 mM $[PtCl_6]^{2-}$. As illustrated in Fig. 1, platinization was performed by reduction of the $[PtCl_6]^{2-}$ in PSI eluate by dihydrogen flowing for ~2 h in the headspace of a reaction vessel that contained the reaction medium. The liquid below the headspace was stirred gently with a Teflon-coated magnetic stirring bar at 20°C, according to the procedure described previously (Greenbaum, 1985). Before and after the platinization, the pH of the samples was monitored using a Beckman 72 pH meter (Beckman Instruments, Inc., Fullerton, CA). As predicted by the platinization reaction, protons were generated in the reduction of $[PtCl_6]^{2-}$ by H_2. To prevent a disruptive pH decrease, the generated protons were buffered by 0.2 M phosphate (pH 7.00) in the reaction medium. Because of the adequate capacity of the phosphate buffer, the platinization process typically resulted in a decrease of ~0.1 pH unit under the assay condition.

STM imaging of PSI-40 particles before and after platinization

STM substrate plates were prepared by evaporation of gold onto freshly cleaved mica at 480°C to form epitaxially grown gold surfaces on the mica.

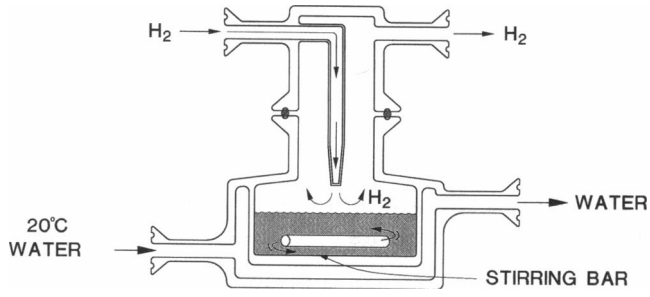

FIGURE 1 Schematic illustration of chemical platinization in PSI solution using $[PtCl_6]^{2-}$. Chemical platinization was performed by reduction of $[PtCl_6]^{2-}$ in a 20°C water-jacketed reaction vessel. The green liquid is the PSI solution containing 2 mM $[PtCl_6]^{2-}$ at pH 7.0. The platinization reaction was driven by a hydrogen flow over the gently stirred liquid sample.

PSI particles were placed on the gold surface by two different techniques: 1) by directly drying a thin layer of platinized or control PSI solution on gold plates; and 2) by "welding" PSI particles onto gold plates by in situ chemical platinization. This in situ welding technique has been described in detail elsewhere (Lee et al., 1995, in press). Briefly, the welding process took place in PSI medium in which a gold plate (~0.5 cm in diameter) was immersed while $[PtCl_6]^{2-}$ was reduced to metallic platinum in the medium at 20°C by H_2 flow. The metallic platinum formed under biologically compatible conditions has a binding affinity for both PSI and gold, resulting in PSI-platinum-gold anchoring. The PSI-anchored gold plates were then washed 4 times by rinsing and soaking each in 100 ml of double-distilled water before drying them in air for STM imaging.

The technique of PSI particle imaging has been described in detail elsewhere (I. Lee et al., 1995). Briefly, a NanoScope-III STM (Digital Instrument, Inc., Santa Barbara, CA) was used in a constant-current mode with 500- to 600-mV bias voltage between substrate and tip (with the scanning tip grounded), 160- to 200-pA tunneling current, and 2- to 4-Hz scan rate. The STM was calibrated with a gold calibration ruling supplied by the STM manufacturer so that the relative error of size measurements was within 3%.

After PSI images were obtained, the size of PSI particles was measured by using the software for quantification of surface properties provided for the NanoScope. By using this software, a cross sectional profile of a PSI image can be displayed and distinguished from the substrate by its sharply rising edge. For the size measurements, the edge of a PSI particle was defined by the boundary where the cross sectional line starts rising.

Time-resolved fluorescence decay kinetics measurements

Fluorescence decay kinetics in platinized and control PSI samples were measured using the technique of picosecond time-resolved single-photon counting (Chang et al., 1985; Owens et al., 1987, 1988). For the measurements, the samples were diluted by a factor of four with 10 mM phosphate buffer. Approximately 4 ml of diluted sample was placed in a standard 1 × 1 × 4 cm fluorescence cuvette and stirred with a small magnetic stirring bar at room temperature during the fluorescence lifetime measurement. The excitation (660 nm) pulses were provided by a synchronously pumped, DCM dye laser that was cavity-dumped at 3.8 MHz. The full width at half-maximum (FWHM) of the pulses was 11 ± 2 ps. The excitation beam was attenuated with neutral density filters so that the maximum excitation intensity was no greater than 3×10^{-4} photons absorbed per PSI complex per pulse (which is well below the threshold for annihilation). Fluorescence was collected at 90° to the excitation beam through a 0.25-mm slit in the cuvette holder, selected at 680 nm with a monochromator (1-nm bandwidth), and detected by a 12-μm microchannel plate photomultiplier (Hamamatsu R2809U) operated at 3000 V and

−40°C. The instrument response function was obtained by collection of scattered light from a cuvette filled with a low concentration of a neutral scatterer and typically had an FWHM of 60–70 ps. The performance of the laser system was checked by fitting the standard fluorescence decay of oxazine-725 in water.

P700 photooxidation and P700$^+$ reduction kinetics measurements

Kinetics of P700 photooxidation under weak actinic illumination and P700$^+$ reduction in darkness were measured in the presence of 20 mM ascorbate and 1 mM methyl viologen by monitoring the absorbance change at 697 nm with a laboratory-built modulated absorbance spectrophotometer (Zipfel and Owens, 1991; Lee et al., 1992; Lee, 1993). The weak actinic illumination (30 μE m^{-2} s^{-1}) was provided by a 150-W dichroic reflector halogen lamp projected through a CS4–96 broadband blue filter and neutral density filters. The actinic intensity was measured using an IL-1700 light meter (International Light, Inc., Newburyport, MA) with a calibrated detector. The platinized and control PSI samples were diluted by a factor of 2 with 10 mM phosphate (pH 7.0) and placed in a cuvette with a path length of 10 mm along the measuring axis and 5 mm along the actinic axis. P700 photooxidation kinetics data were normalized to the full extent (A_{697}^{max}) of the P700 bleach under high actinic intensity (156 μE m^{-2} s^{-1}) and fit to a sum of simultaneous exponential components:

$$\frac{\Delta A_{697}(t)}{\Delta A_{697}^{max}} = A_1(1 - e^{-k_1 t}) + A_2(1 - e^{-k_2 t}), \qquad (1)$$

using standard nonlinear least-squares analysis (Zipfel and Owens, 1991). A_1 and A_2 and k_1 and k_2 are parameters determined by the kinetics. The product of A_1 and k_1 is known to represent the light-dependent rate constant of P700 photooxidation (Lee, 1993).

The kinetic curve of P700$^+$ reduction in darkness was fit to a sum of two exponential decays with amplitudes A_{r1} and A_{r2} and rate constants k_{r1} and k_{r2}:

$$\frac{\Delta A_{697}(t)}{\Delta A_{697}^{max}} = A_{r1}e^{-k_{r1}t} + A_{r2}e^{-k_{r2}t}. \qquad (2)$$

RESULTS AND DISCUSSION

STM examination of PSI-40 with and without platinization

STM examination revealed that the PSI preparation contained pure monomeric PSI particles, in contrast to the PSI samples of several other investigators, which included detectable trimeric aggregates because they were prepared with other detergents and different techniques (Boekema et al., 1989; Rogner et al., 1990; Tsiotis et al., 1993). We found that an appropriately small amount (0.05%) of Triton is essential to suspend PSI particles and prevent aggregation in the phosphate buffer (pH 7.0) at room temperature (20°C). As visualized using STM without any metallic coating, the shape of these monomeric PSI particles (pointed out by *arrows* in Fig. 2 *A*) was roughly ellipsoidal and similar to PSI images previously obtained by electron microscopic analysis (Boekema et al., 1990). Phosphate crystallites that precipitated (probably with a small amount of Triton X-100) during drying of the liquid PSI samples on the gold surface can be distinguished from the ellipsoidal PSI particles (Fig. 2 *A*).

According to the size measurements with STM, the length (major axis) and width (minor axis) of bare PSI particles were ~6 and 5 nm, respectively (Table 1). After platinization the PSI particles generally became larger, due to the presence of metallic platinum precipitated on PSI during the platinization (Fig. 2 *B*). The average size was 9 × 7 nm for platinized PSI particles. This size increase is evidence that metallic platinum formed by the platinization reaction at room temperature has binding affinity for isolated PSI particles. According to a simple calculation based on the size difference between platinized PSI and control PSI, there were probably ~1000 platinum atoms bound on each platinized PSI particle. The binding is probably through image-charge force between PSI and metallic platinum, because it is known that PSI particles carry surface charges.

In theory, an ideal STM image requires a perfectly conducting sample, because the height (thus, the image) of a sample is sensed by the tunneling current between the scanning tip and the sample. PSI is a pigment-protein complex, which is not a perfect conductor. Interestingly enough, such a biomolecular object can be seen, however, clearly on gold substrate without any metallic coating (Fig. 2 *A*). Guckenberger and co-workers have also provided dramatic illustrations in which the STM, nominally limited to imaging good conductors, can, in fact, obtain images on insulating surfaces under certain conditions (Guckenberger et al., 1994). Our studies with tunneling conductance measurements (I. Lee et al., 1995) demonstrated that PSI is not an absolute insulator, but a semiconductor with an energy gap of 1.8 eV when PSI is oriented with its vectorial electron transport chain parallel to the gold surface (Lee et al., 1995). The 1.8 eV matches the energy level of the first excited singlet state of chlorophyll in PSI. Therefore, the semiconducting-like property of PSI is a characteristic of the pigment-protein complex.

The electrical properties of a sample can also be revealed by STM imaging. We observed that the average height of STM images for bare PSI particles was ~0.45 nm, which is ~10% of the known height for PSI, because of the semiconducting properties of PSI that cause the scanning tip to move much closer toward the PSI particle than would be expected for a perfect conducting sample at the constant-current STM operating mode. The STM image of platinized PSI particles (Fig. 2 *B*) displayed a similar height (0.50 nm). This result indicated that the colloidal metallic platinum did not form a completely conductive shell coating on these platinized PSI particles when they were placed over the gold surface.

A complete platinum coating of PSI particles, however, was obtained when PSI particles were anchored in situ on gold plates using the platinization "welding" technique, a second method of placing PSI particles on STM substrates. The thickness of the platinum film can be controlled by the degree of platinization. When the colloidal platinum film reaches a thickness of ≥1–2 nm, a stable conductive coating is likely obtained over PSI particles. Fig. 3 presents an STM

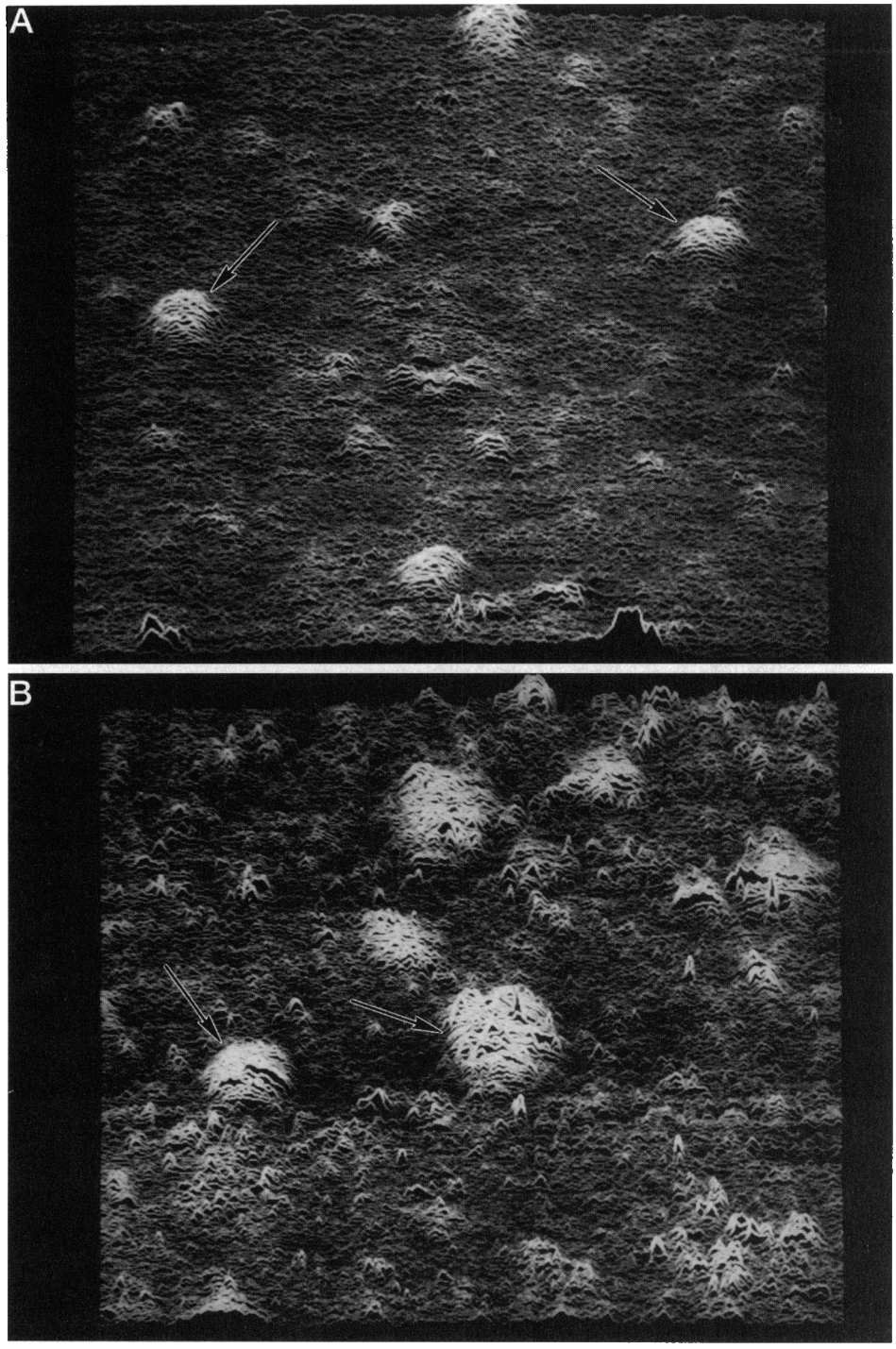

FIGURE 2 STM images of control (*A*) and platinized (*B*) photosystem I (PSI) samples. The images shown are three-dimensional topographical surfaces in a 40 × 40 nm area at a viewing angle of 60°. Both platinized and control PSI solutions were applied directly onto the gold plates as a thin liquid film and dried in air before visualization by STM. Ellipsoidal objects are bare PSI particles (pointed out by *arrows* in *A*). Platinized PSI particles (*B*) are generally larger than bare PSI particles (*A*), although the colloidal platinum did not form a complete conductive coating on the platinized PSI.

image of PSI particles with such a conductive platinum coating. The platinum film on these PSI particles provided a good conducting surface in connection with the gold substrate, resulting in an excellent STM image, which displayed real three-dimensional shape of PSI complexes—all ellipsoidal in shape. In this STM image, a true three-dimensional size was obtained for the platinum-coated PSI complex: length (10 ± 0.8 nm), width (7 ± 0.8 nm), and height (7 ± 0.8 nm). The size variation (±0.8 nm) here is most likely due to the variation in thickness of the platinum films on PSI particles. Surprisingly, the size measurement of these completely coated PSI particles was fairly consistent with the size information obtained from STM images of bare PSI (6 × 5 nm) and (partially) platinized PSI (9 × 7 nm), the height of which was "compressed" by their semiconducting property (Fig. 2, *A* and *B*). The size of a bare PSI should be the size of a platinum-coated PSI minus the thickness of the coating. The STM image of the metal-coated PSI gave an upper limit of PSI size. On the other hand, an STM image of bare PSI provided a lower limit of

TABLE 1 Sizes of photosystem I reaction center/core antenna complexes (PSI) before and after chemical platinization

PSI	Major axis (nm)	Minor axis (nm)
Before platinization	5.9 ± 0.4	4.9 ± 0.4
After platinization	8.8 ± 1.2	7.1 ± 1.2

The sizes of PSI were measured directly with scanning tunneling microscopy. The shape of PSI particles was roughly ellipsoidal. Major and minor axes were measured as the maximal length and width of the particles, respectively. The SDs were calculated from measurements of 60 PSI particles from four independent samples.

PSI size, because the effect of the height "compression" may underestimate the size somewhat. Therefore, the correct length (major axis) and width (minor axis) of a bare PSI must lie within 6–10 and 5–7 nm, respectively. Boekema et al. (1990) reported previously that size for CPI, a monomeric PSI particle, negatively stained by uranyl acetate, was 15.3 × 10.5 nm, which apparently exceeded the upper limit of PSI size we observed in platinum-coated PSI using STM. This variation might be due to some difference in PSI samples. CPI contained ~100 chls/P700 (Boekema et al., 1990), whereas our PSI particles contained ~40 chls/P700. Alternatively, it suggests that the staining by uranyl acetate enlarges the PSI size more than does a thin coating of platinum atoms. Our size analysis also supported the statement that the PSI particles in our samples were exclusively monomeric, because our PSI size (8 × 6 nm) would be too small for trimeric or dimeric PSI clusters.

Effect of platinization on excitation transfer dynamics

The excitation lifetime within a coupled PSI reaction center/core antenna complex is limited by the photochemistry in the reaction center (Owens et al., 1987, 1988). If the platinization caused the release of antenna chls from the PSI-40 complex or if it damaged P700, we would expect in both cases an increase in the amplitude of the nanosecond lifetime component resulting from the presence of chls that are functionally uncoupled from P700. These potential effects of platinization can be easily detected by measuring PSI fluorescence decay kinetics using the technique of picosecond single-photon counting. Fig. 4 presents a typical fluorescence decay measurement in platinized PSI, with instrument response function, along with a three-exponential fit to the data. According to the multi-exponential fits to the data, the fluorescence decay in platinized PSI essentially has the same characteristics as that in control PSI (not shown). Both can be fit by three exponential components (X^2 = 1.01) but not by two exponential decays (X^2 = 2.8). Addition of a fourth exponential component did not significantly improve the fit, as judged by the values of X^2 and the distribution of residuals (such as in Fig. 4 *A*). The excitation transfer dynamics measured in both platinized and control PSI can, therefore, be described as a sum of three exponential

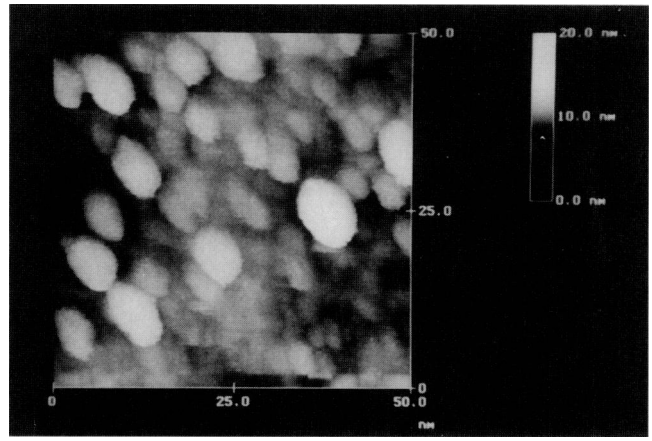

FIGURE 3 STM image of PSI particles that were "welded" onto a gold plate by in situ chemical platinization. A complete and conductive platinum coating was formed over the PSI particles. The metallic coating also made good connection with the STM gold substrate, and a true-height three-dimensional image of PSI particles was obtained. Height was indicated by the 0- to 20-nm height indicator in the 50 × 50 nm two-dimensional image. The image demonstrates that PSI particles are monomeric and ellipsoidal in shape.

decay components (Table 2). The fast (~16 ps) component with a dominant amplitude (0.98) is known to reflect the photochemically limited core excitation decay (Jean et al., 1989; Jia et al., 1992; Zipfel, 1993; Lee, 1993; Laible et al., 1994). No significant change in lifetime or amplitude of the fast component was observed before and

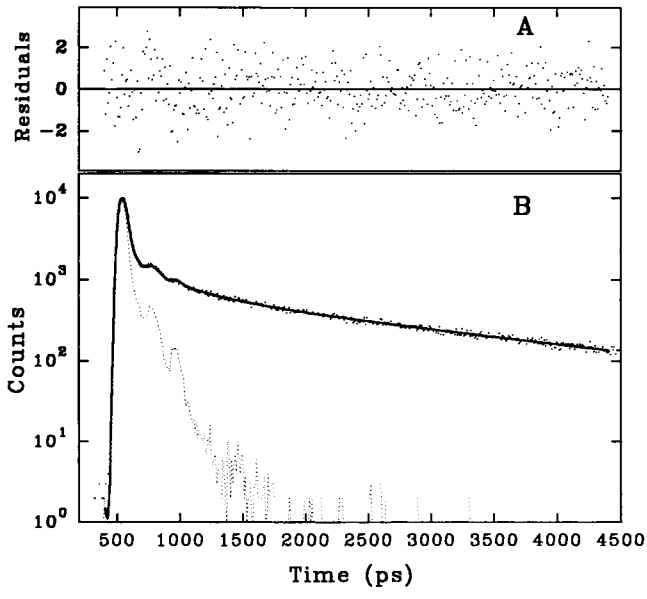

FIGURE 4 Fluorescence decay kinetics of platinized PSI-40 measured with the technique of picosecond single-photon counting. Excitation was at 660 nm, and emission was collected at 680 nm. The data were fit to the weighted sum of three-exponential terms through an iterative convolution with the instrument response function. Plot A is the weighted residuals from the fitting. Plot B contains the data (dots), instrument response function (- - - -), and the fit (——).

TABLE 2 Excitation decay kinetics measured by picosecond time-resolved single-photon counting in control and platinized PSI-40

PSI-40 control		Platinized PSI-40	
Amplitude	Lifetime (ps)	Amplitude	Lifetime (ps)
0.981 ± 0.003	15.8 ± 1.2	0.975 ± 0.003	15.9 ± 1.2
0.009 ± 0.002	510 ± 60	0.014 ± 0.002	400 ± 60
0.010 ± 0.002	3200 ± 350	0.011 ± 0.002	2700 ± 350

Excitation was at 660 nm, and fluorescence emission was collected at 680 nm. The reported SDs, which are due to instrument instability, are the maxima from either the control or platinized samples.

after platinization. Therefore, the platinization essentially caused no damage to the functions of either the reaction center or antenna pigments in PSI complexes. The excitation transfer and trapping in platinized PSI was as efficient as that in control PSI.

The intermediate-lifetime (400–500 ps) and the long-lifetime (>2500 ps) components are likely related to the electron transfer within PSI complexes and to the functionally uncoupled chl, respectively (Zipfel, 1993; Lee, 1993). These components were very small in both the platinized and control PSI samples. The extremely small amplitude (0.01) of the long-lifetime (>2500 ps) component indicated that the amount of functionally uncoupled chls was small in both platinized and control PSI. About 99% of chls are functionally connected to the reaction center P700. Neither the PSI isolation procedure nor the chemical platinization process caused any significant uncoupling of the chls in the PSI complexes. This conclusion was also supported by absorbance spectra of the PSI sample measured before and after platinization (data not shown). It is known that any uncoupling of PSI chls results in a blue-shift in absorbance peaks due to increase in energy level of the chls upon uncoupling. The measurements showed that the PSI absorbance peak at 676 nm remained the same before and after the platinization, which indicated no sign of uncoupling.

Effect of platinization on P700 photooxidation and P700$^+$ reduction kinetics

Another way to examine the effect of platinization on photosynthetic function of PSI particles is by measuring P700 photooxidation and P700$^+$ reduction kinetics. The results of the measurements also demonstrated that both platinized and control PSI were photoactive. The reaction centers (P700) in both samples were able to be photooxidized and recovered (through reduction of P700$^+$ by the added ascorbate) repeatedly, although with slightly different rates in the two samples. Fig. 5 presents a typical set of P700 photooxidation and P700$^+$ reduction curves measured under limiting actinic illumination in the two samples. Before the onset (up arrow) of P700 photooxidation by the continuous actinic illumination, the PSI samples were dark adapted and all reaction centers were in the reduced P700 state. After the onset of actinic illumination, the P700$^+$ population rose

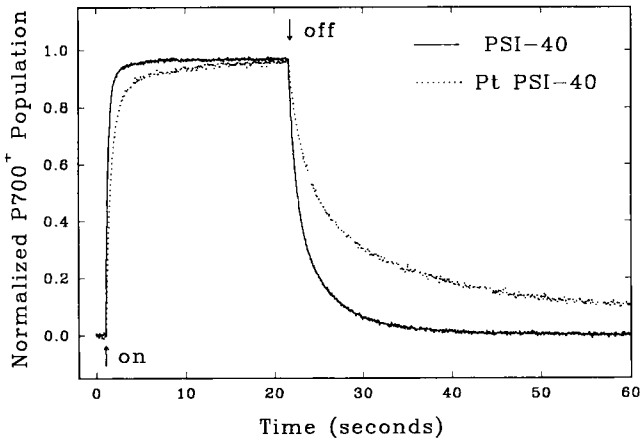

FIGURE 5 A typical set of P700 photooxidation and P700$^+$ reduction curves of platinized and control (without platinization) PSI-40, as measured in the presence of ascorbate, methyl viologen, and O_2. Upward and downward arrows mark the time at which the continuous actinic beam (30 μE m^{-2} s^{-1}) was turned on and off, respectively.

quickly and reached a steady state of P700 photooxidation with O_2 present in the medium as a terminal electron acceptor. The methyl viologen that was added to the medium is known to catalyze the oxidation of the reduced F_{AB}^- by O_2 (Ke, 1972, 1973; Melis, 1982; Lee, 1993). In both samples, the steady-state P700$^+$ population reached ~96% of the total PSI population that was determined by P700 photooxidation at high actinic intensity (156 μE m^{-2} s^{-1}). Based on the efficient P700 photobleach that occurred under limiting actinic illumination, the electrons from F_{AB}^- in the platinized sample must also have been transferred to methyl viologen and/or O_2, presumably through the metallic platinum. The PSI population measured by P700 photooxidation at the high light intensity was identical to that determined by chemically induced absorbance change at 697 nm in both samples. These results indicated that the chemically determined P700 population can be fully photooxidized before and after platinization. Platinization, therefore, does not affect the total active PSI population, which agrees with the results of the fluorescence lifetime study.

When the actinic light was turned off (down arrow), P700 was recovered through the reduction of P700$^+$ by ascorbate in the medium. The reversibility of P700 photooxidation and P700$^+$ reduction is also consistent with the results from the excitation lifetime measurements, which demonstrated that platinization did not cause damage to intrinsic photosynthetic activity of the isolated PSI particles.

The kinetics of P700 photooxidation in both samples were biphasic and could be fit by a sum of two exponential components (Eq. 1). Kinetic parameters (A_1 and k_1, A_2 and k_2) calculated from data fitting are presented in Table 3. The kinetics of P700 photooxidation has been intensively studied (Lee, 1993). According to the previous studies, k_1 and k_2 measure the eigenvalues of three coupled differential equations with five parameters that describe the reversible kinetic system which is contributed not only by the light-

TABLE 3 P700 photooxidation kinetic components in platinized and control PSI-40

PSI-40	A_1	k_1 (s^{-1})	$A_1 \cdot k_1$ (s^{-1})	A_2	k_2 (s^{-1})
Platinized	0.89 ± 0.02	2.6 ± 0.1	2.3 ± 0.1	0.10 ± 0.02	0.18 ± 0.02
Control	0.94 ± 0.02	3.4 ± 0.1	3.2 ± 0.1	0.03 ± 0.02	0.19 ± 0.02

The data were obtained by fitting the P700 photooxidation curves (from the actinic onset point to the point of actinic off, such as illustrated by the upward and downward arrows in Fig. 5) to the kinetic equation (Eq. 1). The kinetics of P700 photooxidation in isolated PSI complexes has been analyzed previously in detail (Lee, 1993). The SDs reported are the maxima from either the control or platinized samples.

limiting P700 photooxidation and charge recombination ($P700F_{AB} \leftrightarrow P700^+F_{AB}^-$) but also by both oxidation of F_{AB}^- ($P700^+F_{AB}^- \rightarrow P700^+F_{AB}$) by exogenous electron acceptors and reduction of $P700^+$ by ascorbate. The two kinetic components are therefore related to all five parameters (reaction steps) and cannot be simply assigned to any of the individual steps. Most importantly, the previous studies also showed that the product $A_1 \cdot k_1$ gives a good approximation of the rate constant of the light-dependent P700 photooxidation (Lee, 1993). Using the product ($A_1 \cdot k_1$) as shown in Table 3, we found that the light-dependent rate constant of P700 photooxidation in platinized PSI (2.3 s^{-1}) was ~30% slower than that in control PSI (3.2 s^{-1}). The only factors that could lead to such a decrease in the rate constant of the light-dependent P700 photooxidation are decreases in 1) the intrinsic quantum yield of photochemistry and/or 2) the rate of actinic photon absorption by PSI (Lee, 1993). As mentioned earlier in the fluorescence lifetime study, the excitation transfer and trapping in platinized PSI was as efficient as that in control PSI. This result indicated that the intrinsic quantum yield of photochemistry was not affected by platinization. Thus, the only possible reason for the decrease in the light-dependent rate constant of P700 photooxidation was a decrease in the rate of actinic photon absorption by PSI. A reduction in the absorbance cross section of PSI by the platinization is unlikely, because platinization did not cause uncoupling of antenna chls and the chl/P700 ratio remained constant before and after platinization. Therefore, this decrease in rate of photon absorption was likely due to actinic shading by platinum, because other factors such as the intensity and wavelength of the actinic illumination were kept constant in the experiments.

According to the typical biphasic kinetics of P700 photooxidation in isolated PSI particles (Lee, 1993), parameter A_2 is expected to increase when the rate of photon absorption by PSI is reduced by platinum actinic shading, whereas parameter k_2 is rather insensitive to the actinic shading. This predicted feature was indeed observed in the current work. The A_2 value (0.10 ± 0.02) in platinized PSI was larger than that in control PSI (0.03 ± 0.02), while the k_2 values in the two samples showed no difference (Table 3). This result also indicated that the platinum affected P700 photooxidation kinetics through its actinic shading.

Another effect of platinum was detected on the rate of $P700^+$ reduction by ascorbate in darkness (after the *down arrow* in Fig. 5). According to data analysis, the reduction kinetics in both samples can be described as a sum of two exponential decays (Eq. 2). The two reduction rate constants (k_{r1} and k_{r2}) differed by a factor of ~4–7, whereas their amplitudes (A_{r1} and A_{r2}) differed only by 10–20%. This result indicated that the electron transfer from ascorbate to $P700^+$ may have two modes. Platinization effected a change in both of the components. In control PSI, A_{r1}, k_{r1}, A_{r2}, and k_{r2} were 0.55, 0.74 s^{-1}, 0.45 and 0.17 s^{-1}, whereas those in platinized PSI were 0.57, 0.32 s^{-1}, 0.39 and 0.044 s^{-1}, respectively. In platinized PSI, the amplitude-weighted rate constant of $P700^+$ reduction ($A_{r1} \cdot k_{r1} + A_{r2} \cdot k_{r2} = 0.20 \pm 0.02$ s^{-1}) was about 2 times slower than that (0.48 ± 0.04 s^{-1}) in the control sample. The decrease in the rate constant of $P700^+$ reduction can be explained by a shielding effect of the metallic platinum covering positively charged sites (such as the plastocyanin (PC) docking site) of PSI complexes, making it less favorable for ionized ascorbate (negative charged) to donate electrons to $P700^+$ through those sites. Previous studies (Greenbaum, 1985; Lee et al., 1994) have shown that negatively charged species (such as $[PtCl_6]^{2-}$) interact preferably with a positively charged site on the reducing side of PSI and that metallic platinum covering the site could limit electron transport from PSI to a negatively charged species by shielding. The exact pathway for ascorbate to donate electrons to $P700^+$ in isolated PSI has not been established. The observed effect of metallic platinum on the $P700^+$ reduction suggests that the electron donation to $P700^+$ by ascorbate may be through some positively charged site(s), such as the PC docking subunit of PSI.

CONCLUSION

In conclusion, chemical platinization at the natural/unnatural (Hoffmann, 1990) interface is applicable to isolated PSI particles. The presence of platinum on platinized PSI particles can be detected by its effects of actinic shading and electronic shielding on P700 photooxidation and $P700^+$ reduction kinetics, in addition to direct visualization by STM. The PSI complexes remained photoactive before and after the chemical platinization. The excitation transfer and trapping dynamics in platinized PSI was as efficient as that in control PSI. These results provided strong evidence that platinization is safe to intrinsic photochemical activity of PSI particles. Chemical platinization has potential as a new technique for building photosynthetic reactors and/or biomolecular optoelectronic devices.

The authors thank D. J. Weaver for secretarial assistance and A. J. Shelton for editorial assistance.

This research was supported by the U.S. Department of Energy. J. W. Lee and I. Lee are postdoctoral fellows appointed to the Oak Ridge National Laboratory Postdoctoral Research Associates Program administered jointly by the Oak Ridge Institute for Science and Education and Oak Ridge National Laboratory. Oak Ridge National Laboratory is managed by Martin Marietta Energy Systems, Inc., for the U.S. Department of Energy under contract DE-AC05-84OR21400.

REFERENCES

Boekema, E. J., J. P. Dekker, M. Rogner, I. Witt, and M. Heel. 1989. Refined analysis of the trimeric structure of the isolated photosystem I complex from the thermophilic cyanobacterium *Synechococcus* sp. *Biochim. Biophys. Acta.* 974:81–87.

Boekema, E. J., R. M. Wynn, and R. Malkin. 1990. The structure of spinach Photosystem I studied by electron microscopy. *Biochim. Biophys. Acta.* 1017:49–56.

Chang, M. C., S. H. Courtney, A. J. Cross, R. J. Gulotty, J. W. Petrich, and G. R. Fleming. 1985. Time-correlated single photon counting with microchannel plate detectors. *Anal. Inst.* 14:433–464.

Golbeck, J. H., and D. A. Bryant. 1991. Photosystem I. *Curr. Top. Bioenerg.* 16:83–177.

Greenbaum, E. 1985. Platinized chloroplasts: a novel photocatalytic material. *Science.* 230:1373–1375.

Greenbaum, E. 1988. Interfacial photoreactions at the photosynthetic membrane interface: an upper limit for the number of platinum atoms required to form a hydrogen-evolving platinum metal catalyst. *J. Phys. Chem.* 92:4571–4574.

Greenbaum, E. 1989. Photobioelectronic studies with thylakoid membranes. *Appl. Biochem. Biotechnol.* 20/21:813–823.

Greenbaum, E. 1992. Kinetic studies of interfacial photocurrents in platinized chloroplasts. *J. Phys. Chem.* 96:514–516.

Guckenberger, R., F. T. Arce, A. Hillebrand, and T. Hartmann. 1994. Imaging of uncoated TMV by scanning tunneling microscopy. *J. Vac. Sci. Technol.* B12:1508–1511.

Hitchens, G. D., T. D. Rogers, O. J. Murphy, and C. O. Patterson. 1991. A new photocatalytic material based on algal cell. *Biochem. Biophys. Res. Commun.* 175:1029–1035.

Hiyama, T., and B. Ke. 1972. Difference spectra and extinction coefficients of P700. *Biochim. Biophys. Acta.* 267:160–170.

Hoffmann, R. 1990. Natural/unnatural. *NER/BLQ.* 12:322–335.

Jean, J. M., C. Chan, G. R. Fleming, and T. G. Owens. 1989. Excitation transport and trapping on spectrally disordered lattices. *Biophys. J.* 56:1203–1215.

Jeffery, S. W., and G. F. Humphrey. 1975. New spectrophotometric equation for determining chlorophylls *a, b, c1* and *c2* in algae, phytoplankton and higher plants. *Biochem. Physiol. Pflanz.* 167:191–194.

Jia, Y., J. M. Jean, M. M. Werst, C. Chan, and G. R. Fleming. 1992. Simulations of the temperature dependence of energy transfer in the PSI core antenna. *Biophys. J.* 63:259–273.

Katz, E. Y., A. Y. Shkuropatov, O. I. Vagabova, and V. A. Shuvalov. 1989. Coupling of photoinduced charge separation in reaction centers of photosynthetic bacteria with electron transfer to a chemically modified electrode. *Biochim. Biophys. Acta.* 976:121–128.

Ke, B. 1972. One-way electron discharge subsequent to the photochemical charge separation in photosystem I. *Biochim. Biophys. Acta.* 267: 595–599.

Ke, B. 1973. The primary electron acceptor of photosystem I. *Biochim. Biophys. Acta.* 267:595–599.

Krauss, N., W. Hinrichs, I. Witt, P. Fromme, W. Pritzkow, Z. Dauter, C. Betzel, K. Wilson, H. T. Witt, and W. Saenger. 1993. Three-dimensional structure of system I of photosynthesis at 6 Å resolution. *Nature.* 361:326–331.

Laible, P. D., W. Zipfel, and T. G. Owens. 1994. Excited-state dynamics in chlorophyll-based antennae: the role of transfer equilibrium. *Biophys. J.* 66:844–860.

Lee, I., J. W. Lee, R. J. Warmack, D. P. Allison, and E. Greenbaum. 1995. Molecular electronics of a single photosystem I reaction center: studies with scanning tunneling microscopy and spectroscopy. *Proc. Natl. Acad. Sci. USA.* In press.

Lee, J. W., W. Zipfel, and T. G. Owens. 1992. Quenching of chlorophyll excited states in photosystem I by quinones: Stern-Volmer analysis of fluorescence and photochemical yield. *J. Lumin.* 51:79–89.

Lee, J. W. 1993. Excitation Transfer Dynamics and P700 Photooxidation Kinetics in Isolated Photosystem I. Ph.D. dissertation. Cornell University, Ithaca, NY.

Lee, J. W., C. V. Tevault, S. L. Blankinship, R. T. Collins, and E. Greenbaum. 1994. Photosynthetic water splitting: in situ photoprecipitation of metallocatalysts for photoevolution of hydrogen and oxygen. *Energy & Fuels.* 8:770–773.

Lee, J. W., I. Lee, and E. Greenbaum. 1995. Platinization: a novel technique to anchor photosystem I reaction centers onto a metal surface at biological temperature and pH. *Biosensors & Bioelectronics.* In press.

Lemieux, S., and R. Carpentier. 1988. Properties of a photosystem II preparation in a photoelectrochemical cell. *J. Photochem. Photobiol. B Biol.* 2:221–231.

Mann, S., D. D. Archibald, J. M. Didymus, T. Douglas, B. R. Heywood, F. C. Meldrum, and N. J. Reeves. 1993. Crystallization at inorganic-organic interfaces: biominerals and biomimetic synthesis. *Science.* 261: 1286–1292.

Markwell, J. P., J. P. Thornber, and M. P. Skrdla. 1980. Effect of detergents on the reliability of a chemical assay for P700. *Biochim. Biophys. Acta.* 591:391–399.

Melis, A. 1982. Kinetic analysis of P700 photoconversion: effect of secondary electron donation and plastocyanin inhibition. *Arch. Biochem. Biophys.* 217:536–545.

Okano, M., T. Iida, H. Shinohara, H. Kobayashi, and T. Mitamura. 1984. Water photolysis by a photoelectrochemical cell using an immobilized chloroplasts-methyl viologen system. *Agric. Biol. Chem.* 48:1977–1983.

Owens, T. G., S. P. Webb, R. S. Alberte, L. Mets, and G. R. Fleming. 1987. Antenna size dependence of fluorescence decay in the core antenna of photosystem I: estimates of charge separation and energy transfer rates. *Proc. Natl. Acad. Sci. USA.* 84:1532–1536.

Owens, T. G., S. P. Webb, L. Mets, R. S. Alberte, and G. R. Fleming. 1988. Antenna structure and excitation dynamics in photosystem I. I. Studies of detergent-isolated photosystem I preparations using time-resolved fluorescence analysis. *Biophys. J.* 53:733–745.

Reeves, S. G., and D. O. Hall. 1980. Higher plant chloroplasts and grana: general preparative procedures. *Methods Enzymol.* 69:85–94.

Rogner, M., U. Muhlenhoff, E. J. Boekema, and H. T. Witt. 1990. Mono-, di-, and trimeric PS I reaction center complexes isolated from the thermophilic cyanobacterium *Synechococcus* sp. Size, shape and activity. *Biochim. Biophys. Acta.* 1015:415–424.

Sanderson, D. G., E. L. Gross, and M. Seibert. 1987. A photosynthetic photoelectrochemical cell using phenazine methosulfate and phenazine ethosulfate as electron acceptors. *Appl. Biochem. Biotech.* 14:1–19.

Tsiotis, G., W. Nitschke, W. Haase, and H. Michel. 1993. Purification and crystallization of photosystem I complex from a phycobilisome-less mutant of the cyanobacterium *Synechococcus* PCC 7002. *Photosynth. Res.* 35:285–297.

Zipfel, W., and T. G. Owens. 1991. Calculation of absolute photosystem I absorption cross-sections from P700 photooxidation kinetics. *Photosynth. Res.* 29:23–35.

Zipfel, W. R. 1993. Modelling Photon Capture, Excitation Energy Transfer and Electron Transfer in Photosynthesis. Ph.D. dissertation. Cornell University, Ithaca, NY.